



The Abdus Salam
International Centre for Theoretical Physics


United Nations
Educational, Scientific
and Cultural Organization


International Atomic
Energy Agency



SMR.1670 - 4

INTRODUCTION TO MICROFLUIDICS

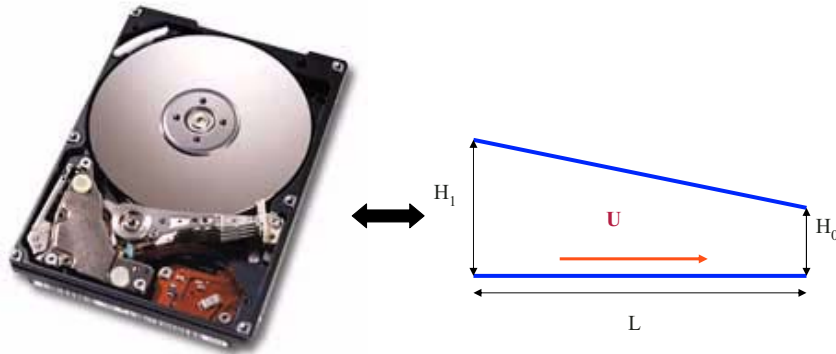
8 - 26 August 2005

Lubrication

Microfilters

A. Beskok
Texas A&M University. U.S.A.

A PHENOMENOLOGICAL MODEL FOR RAREFIED GAS FLOWS IN THIN-FILM SLIDER BEARINGS

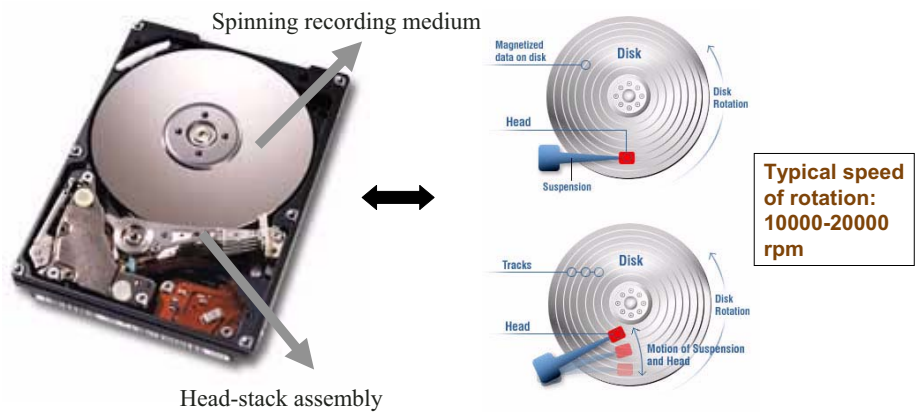


Organization

- Introduction / Motivation
- Specific objectives
- A Modified slip-corrected Reynolds lubrication equation
 - ➡ Governing Equations
 - ➡ Slip Boundary conditions
 - ➡ Poiseuille flow
 - ☑ Velocity and Volumetric flow rate model
 - ➡ Couette flow
 - ☑ Velocity and Shear stress model
 - ➡ Derivation of the slip corrected Reynolds equation
- Lubrication characteristics
 - ➡ Pressure distribution
 - ➡ Bearing load capacity
 - ➡ Velocity profile
 - ➡ Skin friction
- Conclusions and Future Work

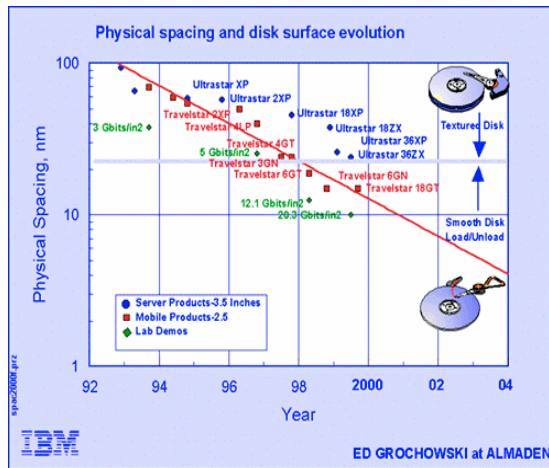
INTRODUCTION

CONFIGURATION OF A COMPUTER HARD DISK DRIVE



- Spinning recording medium.
- Read/write head positioned nano-meters above the spinning platter.
- Thin gas-lubricated film formed between the slider and rotating disk.

RECENT TRENDS IN THE HARD-DRIVE INDUSTRY



GOALS:

- Higher storage densities.
- 12 Gbit/in² → 100 Gbit/in²
- Greater data access speeds.

MEANS:

- Minimize the head-disk spacing.
- Suppress spacing fluctuations during operation.

MODELING CHALLENGES:

Almost all conventional physical models have to be modified to account for new phenomena at this scale.

- **Magnetic spacing** (h_0) becomes comparable to the **mean free path** (λ).
 - Onset of rarefaction
- Small length scales involved → microscopic effects like **slip-length**, **gas surface accommodation**, **surface roughness** etc. become important.

OBJECTIVES:

- Investigate rarefied gas transport in ultra-thin gas lubricating films.
 - Derive a modified slip-corrected Reynolds lubrication equation
 - ➡ Uniformly valid for a wide range of Knudsen numbers and bearing numbers
 - Accurately predict
 - ➡ Velocity profiles
 - ➡ Pressure distribution
 - ➡ Load capacity
 - ➡ Skin friction
- in different rarefaction regions for various slider bearing configurations.

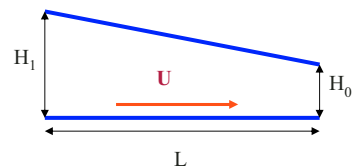
OBJECTIVES (contd..)

- Validate the new model by:
 - Comparisons with the **Direct Simulation Monte Carlo (DSMC)** results available in the literature.
 - Numerical solutions of the uniformly valid **Molecular Gas Lubrication Equation** derived using the **Boltzmann equation**
- Investigate the variation of lubrication characteristics with bearing number and the degree of rarefaction.
- Address some crucial issues in the nano-scale design of computer hard drives.

REYNOLDS LUBRICATION EQUATION

Lubrication: Reynolds Equation

Inertia-free flow if: $\text{Re} \left[\frac{h}{L} \right] \ll 1$



Then, leading-order solution: $\frac{dp}{dx} = \mu \frac{d^2 u}{dy^2}$

Constant flowrate: $\frac{\partial}{\partial X} \left(H^3 P \frac{dP}{dX} \right) = \Lambda \frac{\partial}{\partial X} (PH)$ $\Lambda = \frac{6\mu UL}{p_0 H_0^2}$

Bearing number

\propto Mass flow rate per unit width in plane
Poiseuille flows

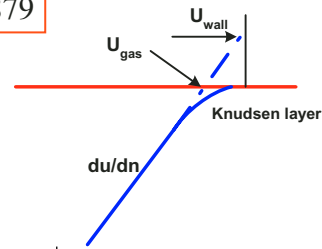
\propto Mass flow rate per unit width in plane
Couette flows

In the absence of thermal creep effects, flow in the lubricating film is a composite of the Poiseuille and Couette flows.

Slip Boundary Conditions

First-order slip boundary condition:

$$\Rightarrow U_g - U_w = \frac{(2-\sigma)}{\sigma} Kn \frac{\partial U}{\partial n} \quad \text{Maxwell 1879}$$



Generalized velocity slip boundary condition:

$$\Rightarrow U_g - U_w = \frac{(2-\sigma)}{\sigma} \left(\frac{Kn}{1-bKn} \right) \frac{\partial U}{\partial n} \quad b = \frac{U_o''}{2U_o'} \Big|_s = -1$$

(Beskok and Karniadakis, 1996)

Plane Poiseuille flow

Momentum equation in the stream-wise direction:

$$\frac{dp}{dx} = \mu \frac{d^2 u}{dy^2}$$

The equation results in the following analytical solution for the velocity profile when subjected to the **generalized velocity slip boundary condition**

$$u_p(y) = -\frac{h^2}{2\mu} \frac{dp}{dx} \left[\frac{2-\sigma_v}{\sigma_v} \frac{Kn}{1+Kn} + \frac{y}{h} - \left(\frac{y}{h} \right)^2 \right]$$

Correction for rarefaction:

➤ The generalized velocity slip model cannot accurately predict velocity profiles and flowrates in the transition and free molecular regimes.

⇒ Navier-Stokes equations **invalid** in this regime.

➤ To account for **increased rarefaction effects**

⇒ The **dynamic viscosity** which defines diffusion of momentum due to intermolecular collisions must be modified.

Generalized diffusion coefficient:

$$\mu(Kn) = \mu_o \left(\frac{1}{1 + \alpha Kn} \right) \quad (\text{Beskok and Karniadakis, 1999})$$

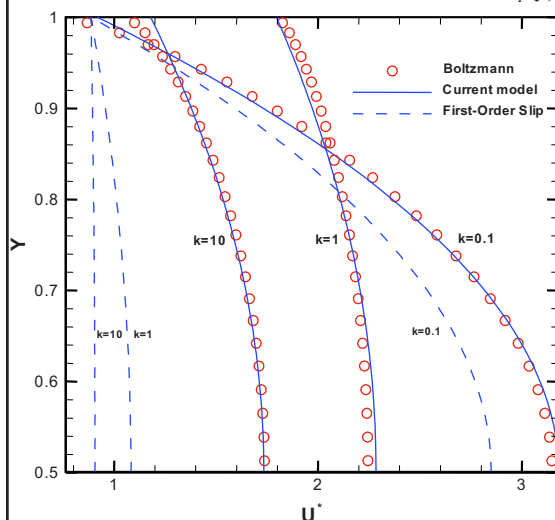
μ_o is the dynamic viscosity

α is a rarefaction correction parameter

Velocity Distribution of Plane Poiseuille Flows

Upper half of the channel is shown

$$u_p(y) = -\frac{h^2}{2\mu} \frac{dp}{dx} (1 + \alpha Kn) \left[\frac{2 - \sigma_v}{\sigma_v} \frac{Kn}{1 + Kn} + \frac{y}{h} - \left(\frac{y}{h} \right)^2 \right]$$



$$k = \left(\sqrt{\pi} / 2 \right) Kn$$

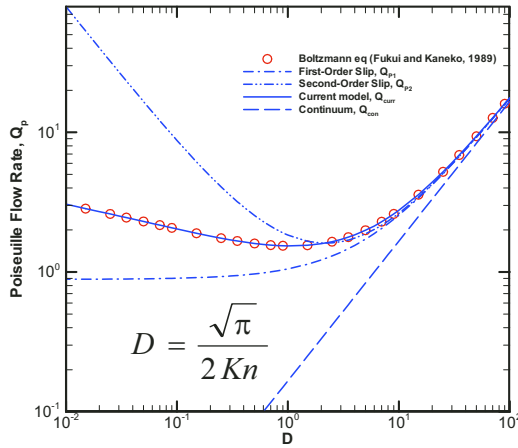
$$U^* = \frac{u_p}{\sqrt{\frac{RT}{2} \frac{h}{P_o} \frac{dp}{dx}}}$$

h : Channel height

P_o : Atmospheric pressure

Model accurately predicts both the magnitude and shape of the velocity profile

Modeling Flowrate



Volumetric Flowrate

$$\dot{Q} = G \left(\frac{dP}{dx}, \mu, h, \lambda \right)$$

Using Navier-Stokes w/ Slip

$$\frac{\dot{Q}}{w} = - \frac{h^3}{12\mu_o} \frac{dP}{dx} \left[1 + \frac{6Kn}{1+Kn} \right]$$

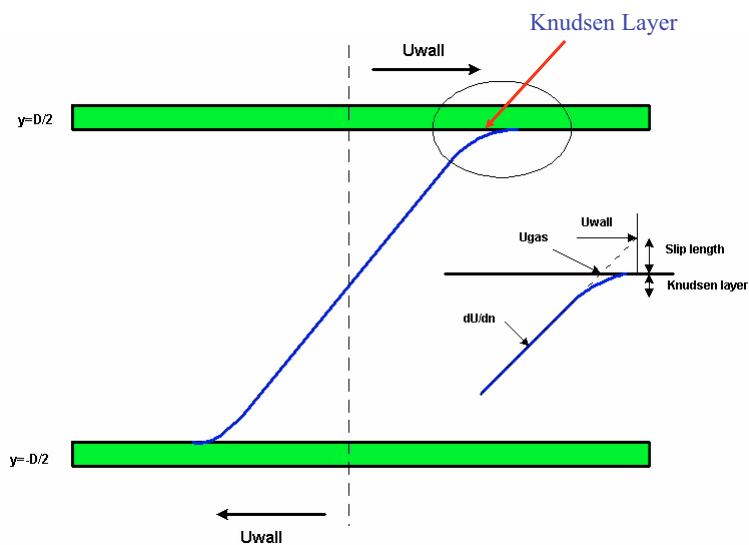
Correct for Rarefaction

$$\frac{\dot{Q}}{W} = - \frac{h^3}{12\mu_o} \frac{dP}{dx} \left[1 + \frac{6Kn}{1+Kn} \right] (1 + \alpha Kn)$$

$$\bar{Q}_P = \frac{Q_P}{Q_{cont}} = \left(1 + \frac{6Kn}{1+Kn} \right) (1 + \alpha Kn)$$

To get $\alpha(Kn, \sigma_v)$: Match the above flow rate model with the Poiseuille flow rate database given by Fukui and Kaneko (1990)

Shear Driven Flows: Linear Couette Flow



Shear Driven Flows: Linear Couette Flow

Governing equation : $\frac{\partial^2 u(y)}{\partial y^2} = 0$ ← Based on Navier Stokes

Boundary conditions :

$$u_g - U_{wall} = \frac{2 - \sigma_v}{\sigma_v} \delta \lambda \left(\frac{\partial u}{\partial \eta} \right)$$

where, δ is the slip coefficient and λ is the mean-free path.

$\delta = 1$ [Maxwell's classical velocity slip formulation]

$\delta = 1.111$ [Obtained by Ohwada et.al. for hard-sphere molecules using the linearized Boltzmann equation]

Analytical expression for the velocity profile (u_c)

$$u_c = \frac{2U_o}{1 + 2 \frac{2 - \sigma_v}{\sigma_v} \delta Kn} \frac{y}{D}$$

where, we have defined $Kn = \lambda/D$.

Generalized Slip coefficient

$$\delta_m = \beta_0 + \beta_1 \tan^{-1}(\beta_2 Kn^{\beta_3})$$

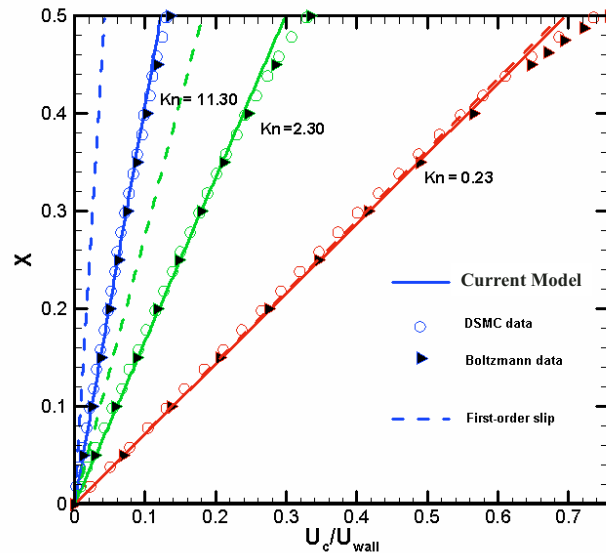
$$\beta_0 = 1.2977; \beta_1 = 0.71851; \beta_2 = -1.17488; \beta_3 = 0.58642$$

(Bahukudumbi and Beskok, 2002)

- Extends the validity of first-order slip condition.
- Converges to the first order slip condition for $Kn < 0.1$.
- Acts as high-order correction for $Kn > 0.1$

Velocity Distribution of Plane Couette Flows

Upper half of the channel is shown



(Bahukudumbi and Beskok, 2002)

Modified Slip-Corrected Reynolds Equation

Velocity profile in the lubricating film:

$$u(y) = u_p(y) + u_c(y)$$

$$u(y) = \underbrace{-\frac{h^2}{2\mu_o} \frac{dp}{dx} (1 + \alpha Kn) \left[\frac{Kn}{1 + Kn} + \frac{y}{h} - \left(\frac{y}{h}\right)^2 \right]}_{\text{Plane Poiseuille flow velocity}} + \underbrace{\frac{U_o(1 + \delta Kn - \frac{y}{h})}{1 + 2\delta Kn}}_{\text{Plane Couette flow velocity}}$$

Mass flow rate:

$$\dot{M} = \underbrace{-\frac{\rho h^3}{12\mu_o} \frac{dp}{dx} (1 + \alpha Kn)}_{\text{Plane Poiseuille Flows}} \left[1 + \frac{6Kn}{1 + Kn} \right] + \frac{1}{2} \rho U_o h$$

Plane Poiseuille Flows

Plane Couette Flows

Note that the mass flow rate of Couette flows is independent of Knudsen number.

Modified slip-corrected Reynolds Equation (contd..)

$$\dot{M} = - \underbrace{\frac{\rho h^3}{12\mu_o} \frac{dp}{dx}}_{\text{Constant}} (1 + \alpha Kn) \left[1 + \frac{6Kn}{1 + Kn} \right] + \frac{1}{2} \rho U_o h$$

Function of x

Taking the gradient of the above equation

$$\frac{\partial}{\partial x} \left(\rho h^3 \frac{dp}{dx} (1 + \alpha Kn) \left(1 + \frac{6Kn}{1 + Kn} \right) \right) = 6\mu_o \frac{\partial}{\partial x} (\rho h U_o)$$

In non-dimensional form:

Modified slip-corrected Reynold's equation

$$\frac{\partial}{\partial X} \left(PH^3 \frac{dP}{dX} (1 + \alpha Kn) \left(1 + \frac{6Kn}{1 + Kn} \right) \right) = \Lambda \frac{\partial}{\partial X} (PH)$$

where, $X = \frac{x}{L}; H = \frac{h}{h_o}; P = \frac{p}{P_a}; \Lambda = \frac{6\mu_o U_o L}{P_a h_o^2}$

Also, local Knudsen number (Kn) = Kn_o/(PH); where Kn_o is the outlet Knudsen number.

Current Model

$$\frac{\partial}{\partial X} \left(PH^3 \frac{dP}{dX} (1 + \alpha Kn) \left(1 + \frac{6Kn}{1 + Kn} \right) \right) = \Lambda \frac{\partial}{\partial X} (PH)$$

Burgdorfer's slip-corrected Reynolds Equation

$$\frac{\partial}{\partial X} \left(PH^3 \frac{dP}{dX} (1 + 6Kn) \right) = \Lambda \frac{\partial}{\partial X} (PH)$$

➤ Can be deduced from the Modified slip-corrected Reynolds equation

○ Set $b = \alpha = 0$

➤ Strictly valid in the slip-flow regime.

LUBRICATION CHARACTERISTICS

LUBRICATION CHARACTERISTICS

- **Pressure distribution and Load capacity**
 - Solve the Modified slip-corrected Reynolds equation.
- **The modified slip-corrected Reynolds equation is**
 - Highly non-linear.
 - Closed form solutions for the most general case do not exist.
- **Solved numerically using a second-order accurate finite difference method.**

FINITE DIFFERENCE FORMULATION

EQUATION:
$$\frac{\partial}{\partial X} \left(PH^3 \frac{dP}{dX} \left(1 + \alpha \frac{Kn_o}{PH} \right) \left(1 + \frac{6Kn_o}{PH + Kn_o} \right) \right) = \Lambda \frac{\partial}{\partial x} (PH)$$

BOUNDARY CONDITIONS: $P(X=0)=1$ and $P(X=1)=1$ $H = H_1(1 - X) + X$

We set $\psi=PH$ and transform the above equation

$$\frac{d}{dX} \left[C_1 H \frac{d\psi}{dX} - (C_2 + \Lambda) \psi \right] = 0$$

$$C_1 = \frac{(\psi + \alpha Kn_o)(\psi + 7Kn_o)}{(\psi + \alpha Kn_o)}, C_2 = C_1(1 - H_1)$$

If the function $\psi(X)$ be expanded about a point X_k using a Taylor's series expansion, we can get the derivatives of ψ at X_k

$$\frac{d\psi}{dX} = \frac{\psi_{k+1} - \psi_{k-1}}{2\Delta X} - \frac{(\Delta X)^2}{6} \psi_{xxx} + \dots$$

$$\frac{d^2\psi}{dX^2} = \frac{\psi_{k+1} - 2\psi_k + \psi_{k-1}}{(\Delta X)^2} - \frac{(\Delta X)^2}{12} \psi_{xxxx} + \dots$$

FINITE DIFFERENCE FORMULATION (contd...)

DISCRETIZED EQUATION:

$$\psi_k^{n+1} = \frac{(\Delta X)^2}{2C_1^n H} \left[\left(\frac{C_1^n H}{(\Delta X)^2} - \frac{(C_2^n + \Lambda - C_1^n(1 - H_1))}{2\Delta X} \right) \psi_{k-1}^n + \left(\frac{C_1^n H}{(\Delta X)^2} + \frac{(C_2^n + \Lambda - C_1^n(1 - H_1))}{2\Delta X} \right) \psi_{k+1}^n \right]$$

- We used N=400 equally spaced grid points in the stream-wise direction. ΔX is the grid spacing=0.0025
- Iterations are continued until the "convergence indicator", is sufficiently small (typically 10^{-14}).
- Grid independence studies were performed.
- Residuals of the global conservation of mass was monitored. $\left| \frac{\psi_k^{n+1} - \psi_k^n}{\psi_k^n} \right|$
- All calculations were performed to double precision accuracy. (16 significant digits)

FINITE DIFFERENCE FORMULATION (contd..)

$$\frac{d}{dX} \left[C_1 H \frac{d\psi}{dX} - (C_2 + \Lambda) \psi \right] = 0$$

$$C_1 = \frac{(\psi + \alpha Kn_o)(\psi + 7Kn_o)}{(\psi + \alpha Kn_o)}, C_2 = C_1(1 - H_1)$$

➤ Above equation is discretized using a second-order accurate finite difference approximation

➤ Resulting set of non-linear equations solved using a **direct iteration/ Picard method**

➤ Iterative method

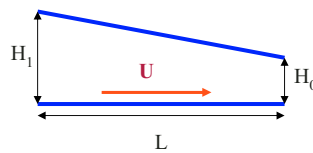
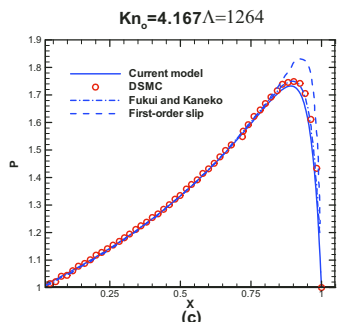
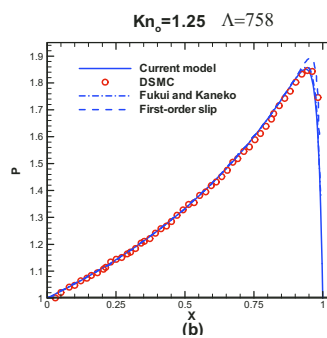
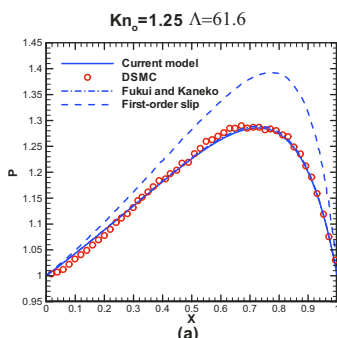
➤ Seeks approximate solutions to the discretized equations by linearization

➤ Initial solution at the start of iteration is important

○ Based on our qualitative understanding of the solution behavior.

○ Solution from a linearized Reynolds equation is used as the initial solution.

Slider Bearing Pressure Distribution

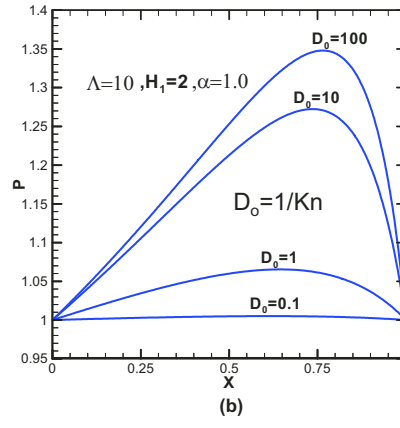
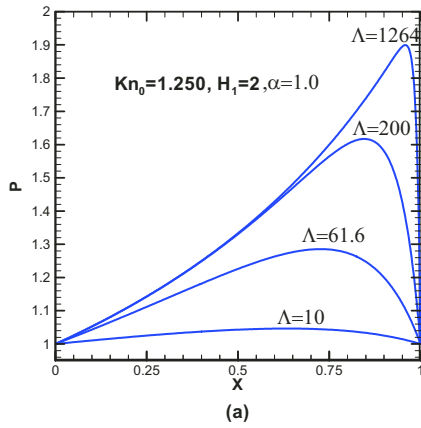


$$\Lambda = \frac{6\mu UL}{p_o H_o^2}$$

$$P = \frac{p}{p_o}, \quad X = \frac{x}{L}$$

Accurate Predictions of Pressure distribution in different rarefaction regions for various Knudsen numbers.

Slider Bearing Pressure Distribution (cont..)

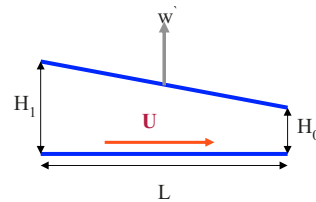
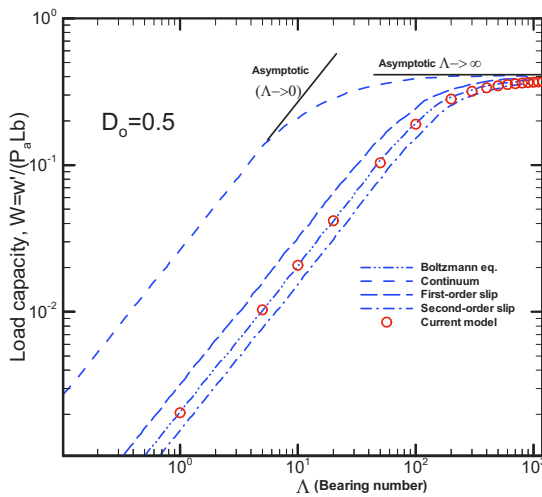


$$\Lambda = \frac{6\mu UL}{p_o H_o^2}$$

$$P = \frac{p}{p_o}, \quad X = \frac{x}{L}$$

Accurate Predictions of Pressure distribution in different rarefaction regions for various Knudsen numbers.

Load capacity as a function of bearing number (Λ)



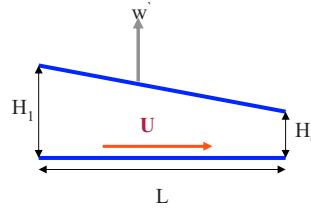
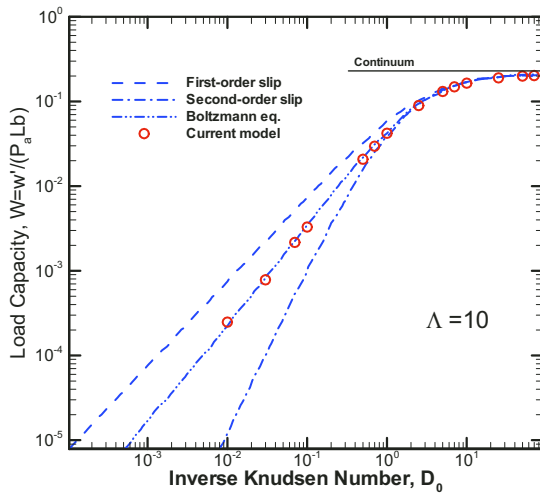
Non-dimensional load capacity:

$$W = \frac{w'}{P_a L b} = \frac{1}{P_a L b} \int_0^1 (P-1) dX$$

Load capacity of the slider bearing:

- Represents vertical load acting on the slider bearing.
- Determines the position of the flying head.
- The head will not accurately read or write if it flies too high and will catastrophically crash into the spinning platter if it flies too low.

Load capacity as a function of Knudsen number



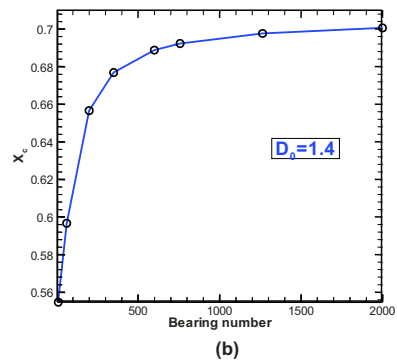
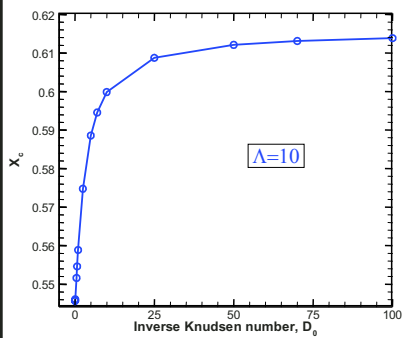
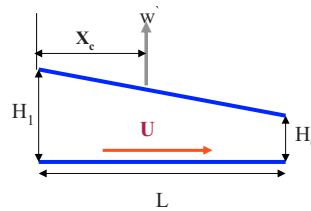
Stream-wise location of the load capacity

$$X_c = \frac{\sum_{i=1}^n (p_i - P_a) X_i}{\sum_{i=1}^n (p_i - P_a)}$$

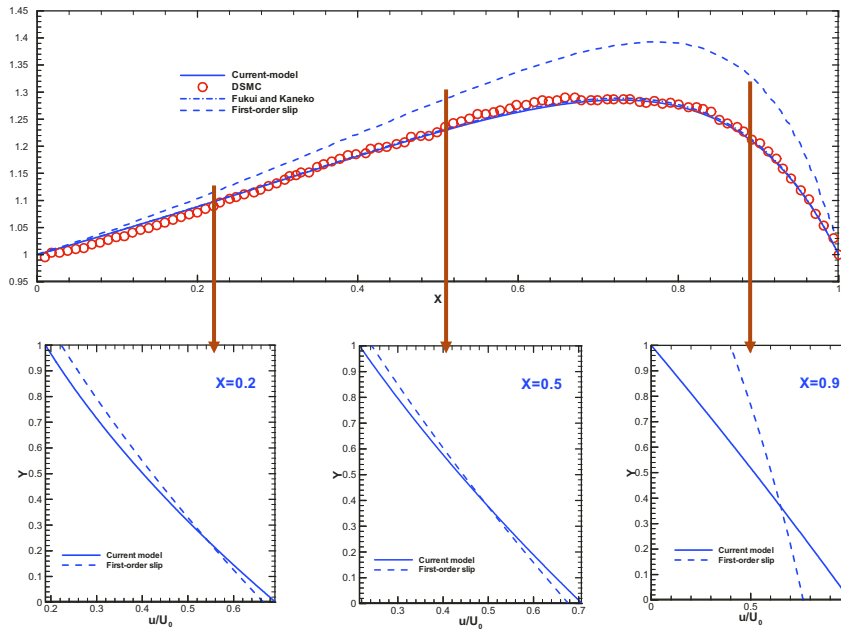
n: Number of cells in the x-direction

i: Cell index

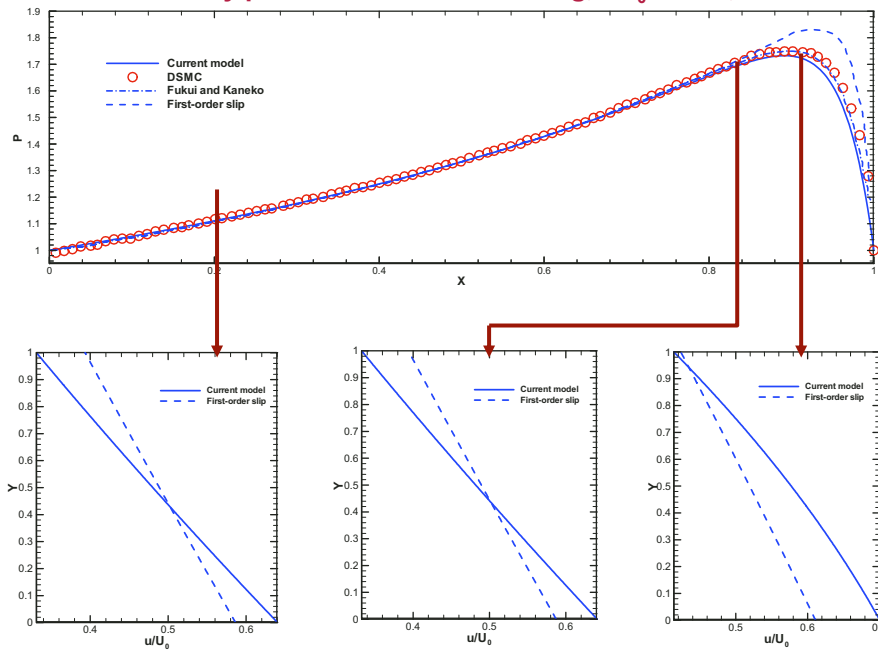
X_i : Location of the i^{th} cell



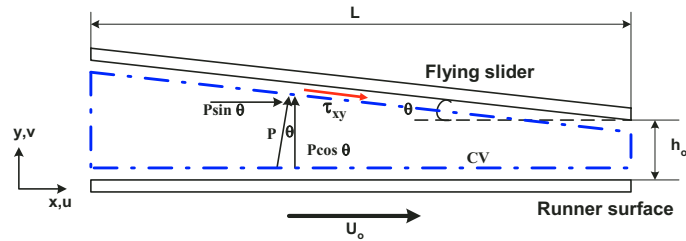
Actual velocity profile in the slider bearing, $Kn_0=1.25$, $\Lambda=61.6$



Actual velocity profile in the slider bearing, $Kn_0=4.167$, $\Lambda=1264$



SKIN FRICTION (SHEAR DRAG):



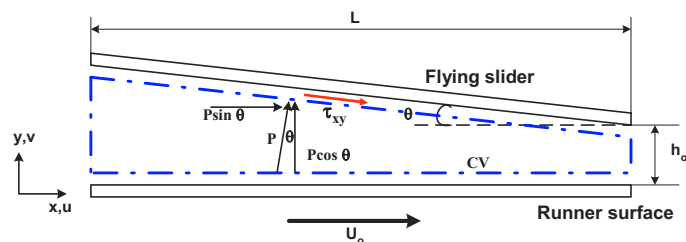
Shear force on the flying slider:

$$dF_x = -\tau_{xy} dA = -(\tau_{couette} + \tau_{Poiseuille}) dA$$

$$\tau_{couette} = -\frac{aKn_o^2 + 2bKn_oPH}{aKn_o^2 + cKn_oPH + b(PH)^2} P_a \frac{U_o}{\sqrt{2RT_w}}$$

$$a = 0.529690; b = 0.602985; c = 1.627666$$

SKIN FRICTION (SHEAR DRAG) (contd.):



$$\tau_{Poiseuille} = \frac{\mu_o}{(1 + \alpha Kn)} \left(\frac{du_p}{dy} \right)_{y=h} \quad Kn = \frac{Kn_o}{PH}$$

$$u_p(y) = -\frac{h^2}{2\mu} \frac{dp}{dx} (1 + \alpha Kn) \left[\frac{2 - \sigma_v}{\sigma_v} \frac{Kn}{1 + Kn} + \frac{y}{h} - \left(\frac{y}{h} \right)^2 \right]$$

Friction Coefficient:

$$C_f = \frac{\tau_{xy}}{\frac{1}{2} \rho U_o^2}$$

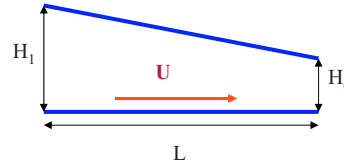
Pressure drag:

$$F_{DP} = \int_0^1 P \sin \theta dX$$

Gas Damping/Lubrication: Reynolds Equation

General equation:

$$\nabla \cdot \left[\left(\frac{\rho h^3}{\mu} \right) \nabla p \right] = 12 \frac{\partial \rho h}{\partial t} + 6 \nabla \cdot (\rho h \vec{U})$$



Inertia-free flow if: $\text{Re} \times \left(\frac{H_0}{L} \right)^2 \ll 1$

Then, leading-order solution: $\frac{dp}{dx} = \mu \frac{\partial^2 u}{\partial x^2}$

Bearing number

• Constant flowrate: $\frac{\partial}{\partial X} \left(H^3 P \frac{dP}{dX} \right) = \Lambda \frac{\partial}{\partial X} (PH) \quad \Lambda = \frac{6\mu UL}{p_0 H_0^2}$

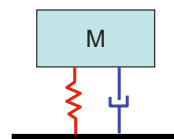
• Slip-Flow: $\frac{\partial}{\partial X} \left(\left[1 + 6 \frac{2 - \sigma_v}{\sigma_v} Kn \right] H^3 P \frac{dP}{dX} \right) = \Lambda \frac{\partial}{\partial X} (PH)$

For generalized model by Fukui & Kaneko, see Karnidakis & Beskok, sec 7.1

Squeezed Film Damping

$$M \frac{d^2 x}{dt^2} + \gamma \frac{dx}{dt} + \kappa x = F_{ext}$$

F_{ext} = driving forces, electrostatic & gas damping forces



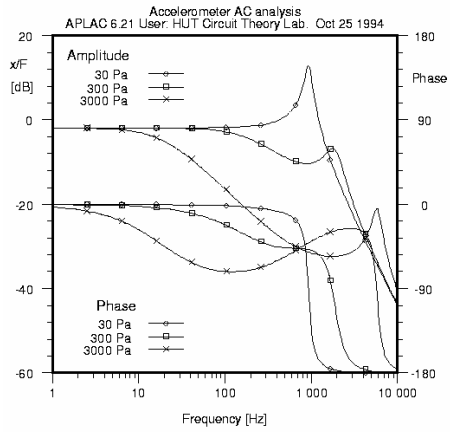
$$\nabla \cdot \left[\left(\frac{\rho h^3}{\mu} \right) \nabla p \right] = 12 \frac{\partial(\rho h)}{\partial t} + 6 \nabla \cdot (\rho h \vec{U}_o)$$

Normal Motion Only

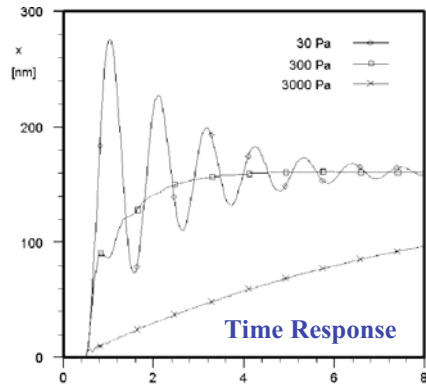
$$\frac{p_0 h^2}{12 \mu_e} \nabla^2 P - \frac{\partial P}{\partial t} = \frac{\partial h}{\partial t}$$

μ_e is an effective viscosity (Veijola et al., 1995)

Squeezed Film Damping



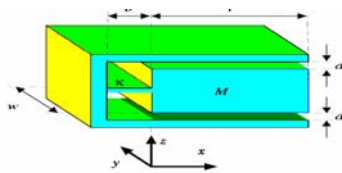
Accelerometer Frequency Response



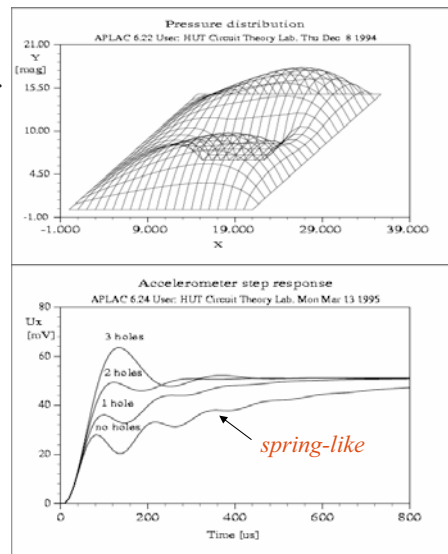
Courtesy of T. Veijola

Coupled Domain Simulations: Squeeze Film Damping

- Titling rectangular accelerometer
- Gap of 2 microns

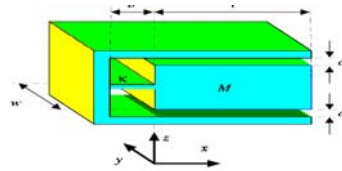
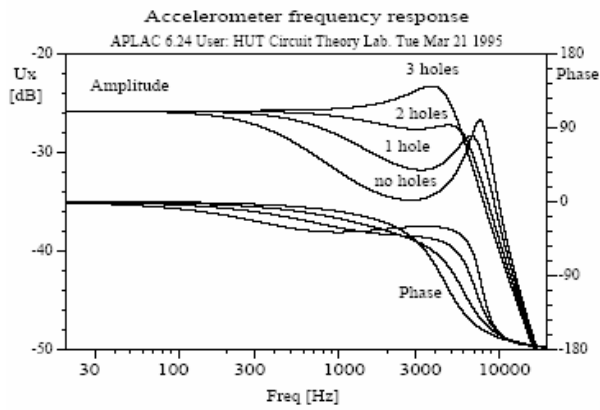


- Generalized Reynolds equation with electrostatic actuation.
- Dynamic response of a micro accelerometer with holes.



Courtesy of T. Veijola

Coupled Domain Simulations: Squeeze Film Damping



CONCLUSIONS:

- Derived a Modified slip-corrected Reynolds lubrication equation valid for:
 - ➡ $0 < Kn < 12$
 - ➡ Low subsonic compressible flows. ($Ma < 0.3$)
 - ➡ Any Bearing Number
- Accurate predictions of
 - ➡ Velocity profiles
 - ➡ Pressure distribution
 - ➡ Load capacity
 - ➡ Shear drag force

CONCLUSIONS (cont..)

➤ Validation by

- Solutions of generalized lubrication equation
- DSMC

➤ Crucial issues in the nano-scale design of computer hard drives

- **Lift force/Load capacity** - Directly related to flying height of slider.
- **Shear drag/ Skin friction** - Accurate modeling of shear drag forces induced by air resistance to track access motion of sliders - required for accurate prediction of ***actuator power consumption***.

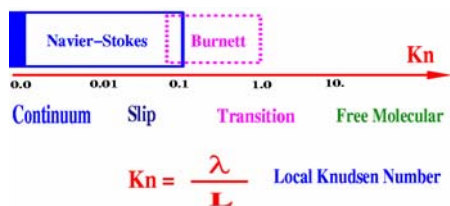
Gas Flow Through Short Channels and Filters

&

External Flows

Gas Transport Modeling

FLOW REGIMES



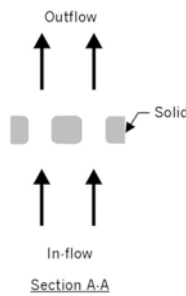
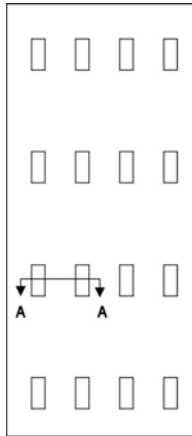
- Continuum & Slip Flow Regimes:
Navier-Stokes Equations
Slip Boundary Conditions

$$U_g - U_w = \frac{(2 - \sigma)}{\sigma} Kn \frac{\partial U}{\partial n}$$

$$T_g - T_w = \frac{2 - \sigma_T}{\sigma_T} \left[\frac{2\gamma}{\gamma + 1} \right] \frac{Kn}{Pr} \left(\frac{\partial T}{\partial n} \right)$$

- Slip, Transitional & Free Molecular:
Direct Simulation Monte Carlo

Micro-Filters



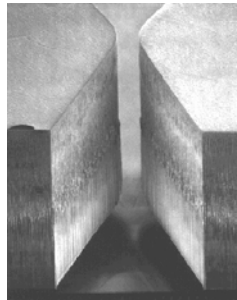
Applications:

Micro-Filters

- Detection of airborne bio/chemical entities
- Environmental monitoring applications

Micro-Nozzles

- Thrust generators for space satellites.



TAMU Micro Fluidics Laboratory

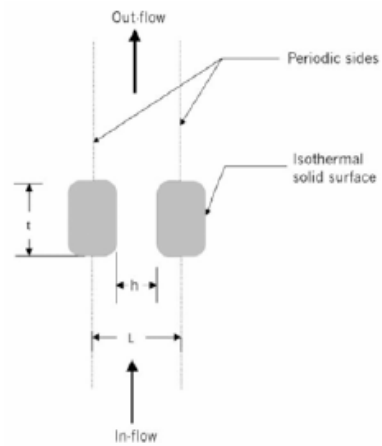
Current Research:-

- Run μ -Flow (*Navier-Stokes solver*) for
 - Variety of micro-constriction geometries and inlet conditions.
 - Determine a fixed aspect ratio for geometric similarity.
- Perform grid independence tests
 - for determining the reliability of the numerical results.
- Perform parametric studies
 - as a function of the Knudsen number, Reynolds number, and the inlet conditions.

TAMU Micro Fluidics Laboratory

Model Details

Lref	Dimensions (micron)		
	L	h	t
6 micron	6	3.6	2.4
4 micron	4	2.4	1.6
2 micron	2	1.2	0.8
1 micron	1	0.6	0.4

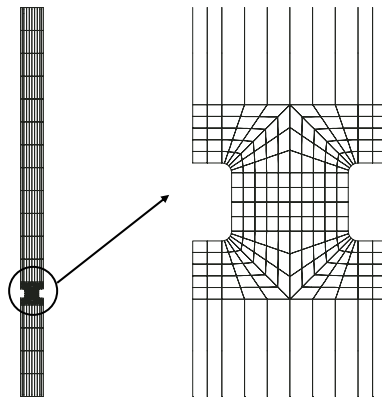


Opening Ratio $\beta = h/L$

TAMU Micro Fluidics Laboratory

Mesh:-

- More concentrated at locations where gradients are expected
- Inlet and Outlet domains have been extended to avoid I/O boundary effects

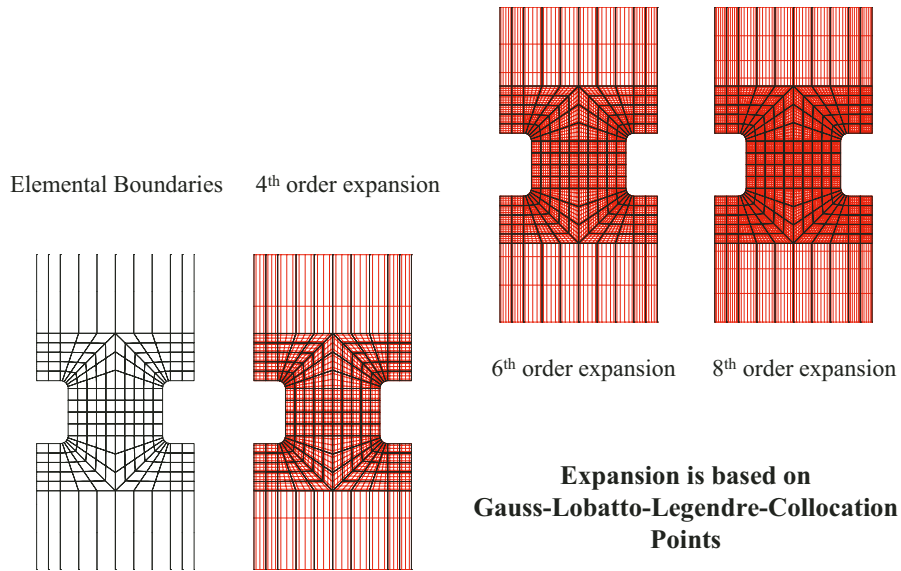


Overall Domain

Grid zoomed at blockage area

TAMU Micro Fluidics Laboratory

Spectral Element Discretization:



TAMU Micro Fluidics Laboratory

Parametric Study:-

Effect of
→ Rarefaction
→ Compressibility
→ Reynolds number

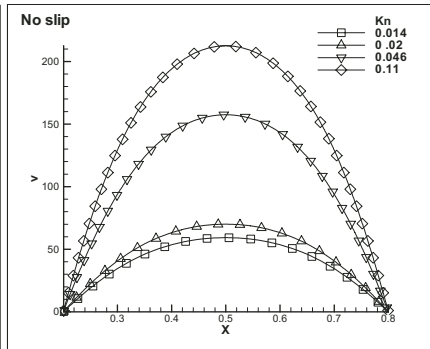
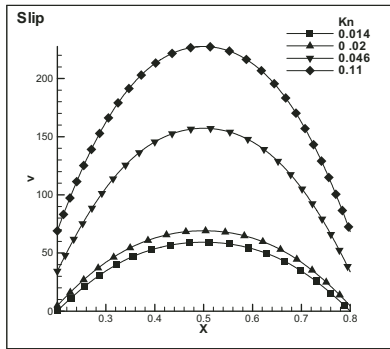
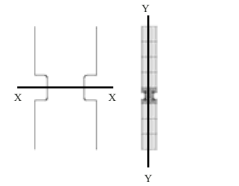
- Local Temperature
- Local Velocity
- Local Density
- Integral Quantities such as;
 - Mass flow rate
 - Drag Force
 - Global Heat Transfer
 - Viscous Heating

TAMU Micro Fluidics Laboratory

Slip:-

(Re ≈ 7.0)

- Inlet velocity is increased
- L is reduced



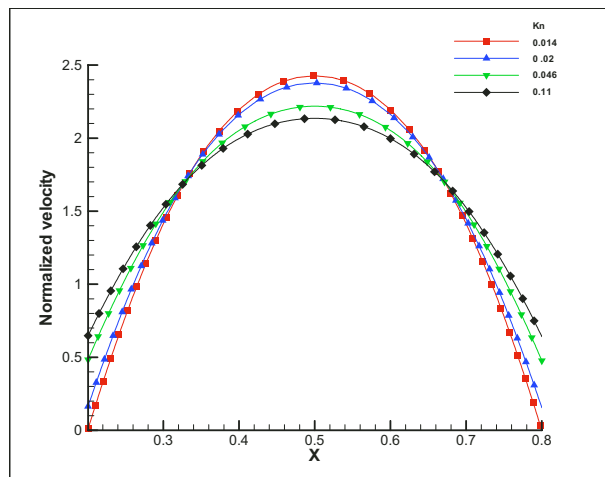
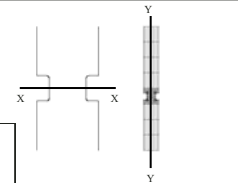
Stream wise Velocity variation along X-X at the middle of blockage

- Finite Slip velocity at the wall due to Rarefaction
- Maximum velocity occurs at mid section, which increases as a result of rarefaction

TAMU Micro Fluidics Laboratory

Rarefaction Effect:-

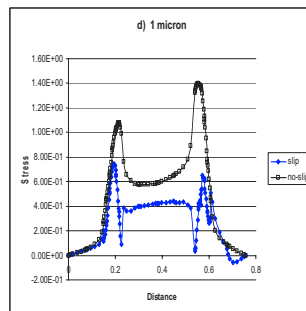
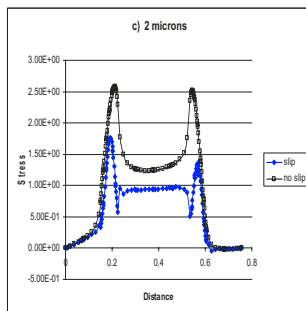
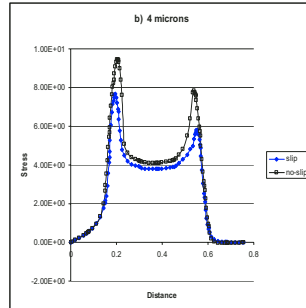
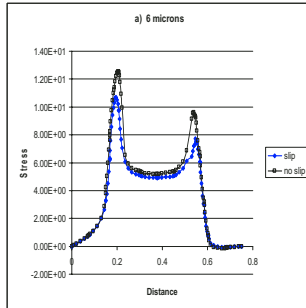
(Re ≈ 7.0)



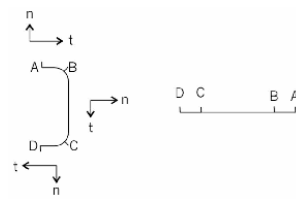
$$u^* = \frac{u}{\bar{u}}$$

- Higher Knudsen number flows have larger slip velocity on the wall, and the velocity profiles are more flattened.
- Flow is not fully-developed.

Rarefaction Effect on Skin Friction

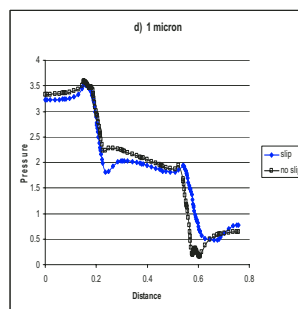
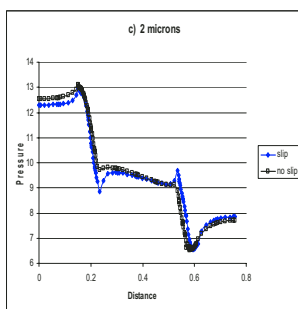
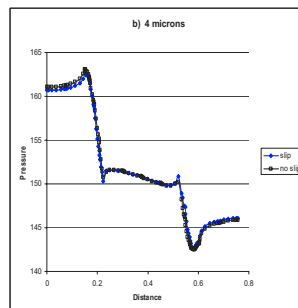
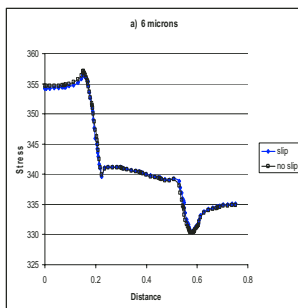


$(Re \approx 7.0)$

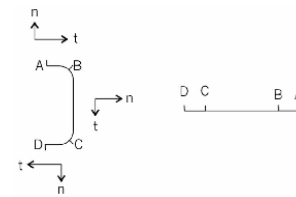


• Shear stresses decrease as a result of rarefaction

Rarefaction Effect on Pressure Distribution

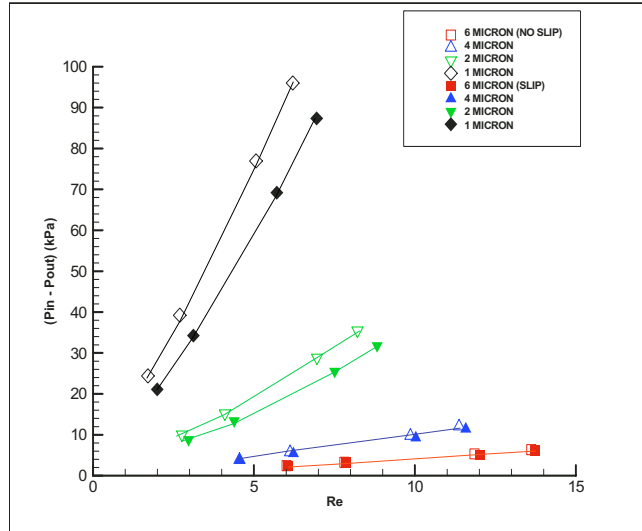


$(Re \approx 7.0)$



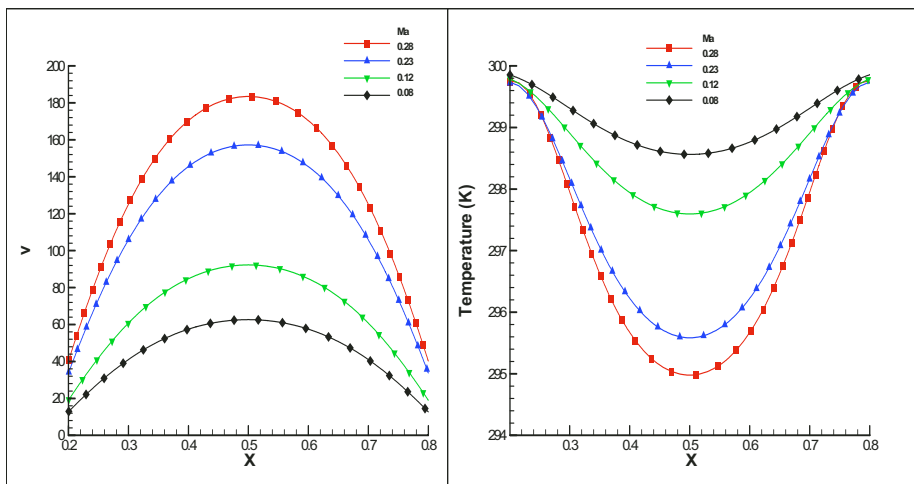
• Reduced pressure difference between the top and bottom surfaces

Rarefaction Effect:-



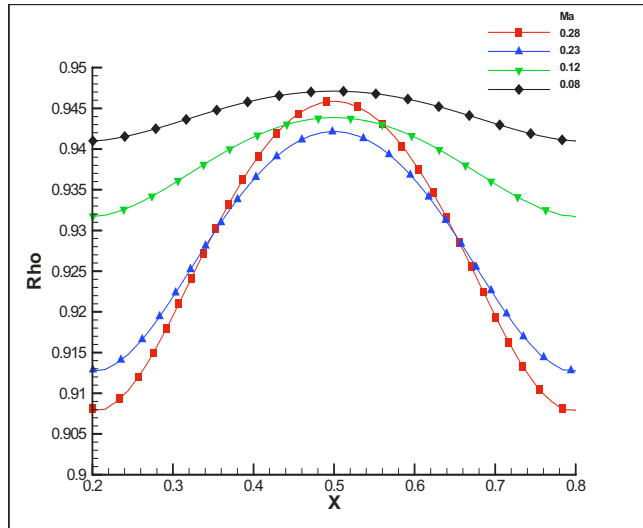
- Pressure drop in slip flows is smaller than the corresponding no-slip cases

Compressibility Effect



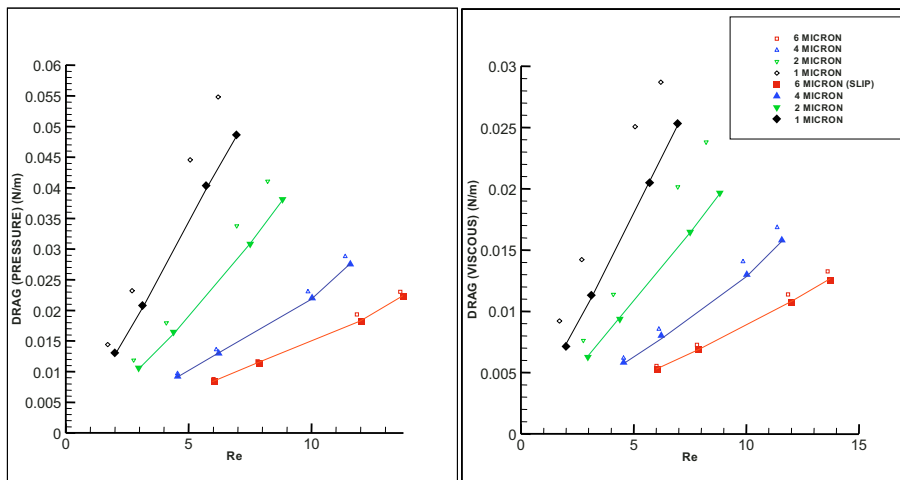
- Maximum velocity is in the middle of the channel and increases substantially with Ma.
- Temperature drops drastically in the middle of the channel for high Mach number cases

Compressibility Effect:-



- Large density variations for high Mach number cases

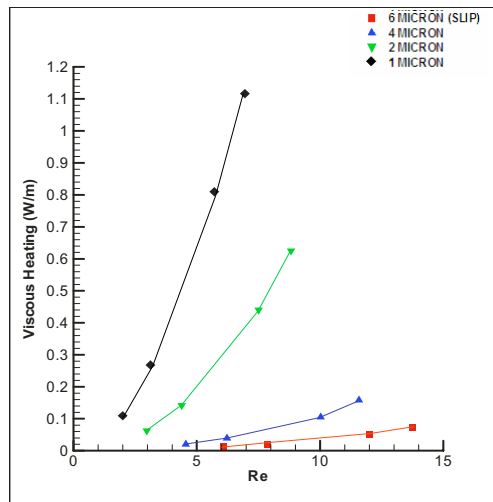
Drag Force



- Drag Reduction due to Rarefaction
- Drag on the body Increases with Reynolds number

- Viscous Forces are about 1/2 in magnitude compared to Pressure forces and hence play key role in design consideration

Viscous Heating:-



$$\int_{CS} (n_j \tau_{ji}) \cdot v_i dS$$

• Viscous heating increases with the Reynolds number

TAMU Micro Fluidics Laboratory

Scaling Laws For Micro Filters

$$\kappa = \beta^{-2} \left(\frac{t}{h} \right)^{0.28} \left(\frac{73.5}{Re} + 1.7 \right),$$

Yang et al., 1999

$$\kappa = \beta^{-2} \left(3.5 \frac{t}{h} + 3 \right) \left(\frac{10}{Re} + 0.22 \right)$$

Yang et al., 2001

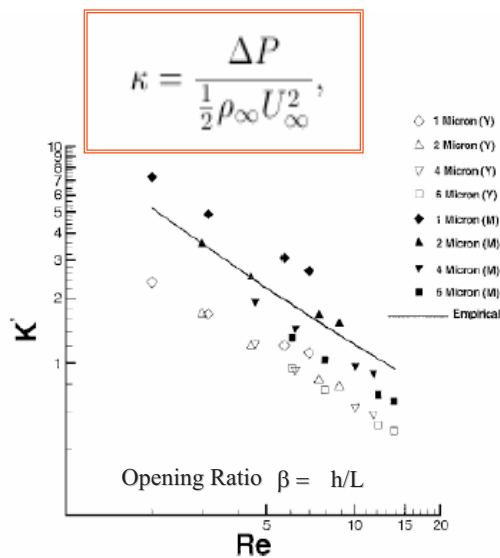
$$\kappa = \beta^{-2} \left(3.5 \frac{t}{h} + 3 \right) \left(\frac{10}{Re} + 0.22 \right) \left[\frac{0.0577}{0.0577 + Kn} \right]$$

Mott et al., 2001

$$\kappa = 2.833 \beta^{-2} \left(\frac{10.0}{Re} + 0.22 \right)$$

Ahmed & Beskok, 2002

$$\kappa = \frac{\Delta P}{\frac{1}{2} \rho_{\infty} U_{\infty}^2}$$

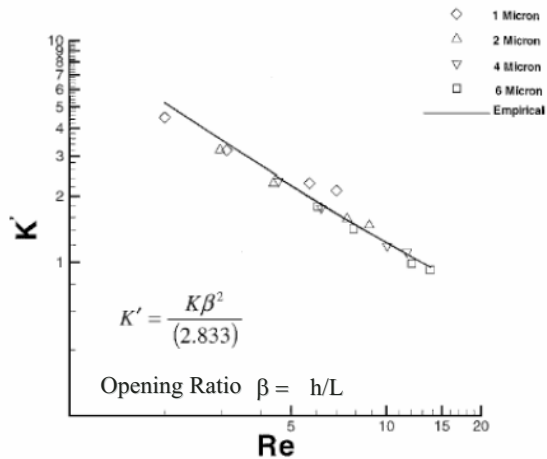


Scaling Laws For Micro Filters

$$\kappa = 2.833\beta^{-2} \left(\frac{10.0}{Re} + 0.22 \right)$$

For general filter geometry, 2.833 should be a function of t/h . Also we expect explicit Kn dependence in a more generalized case.

$$\kappa = \frac{\Delta P}{\frac{1}{2}\rho_{\infty}U_{\infty}^2}$$



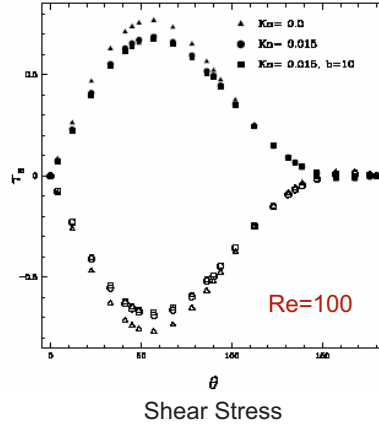
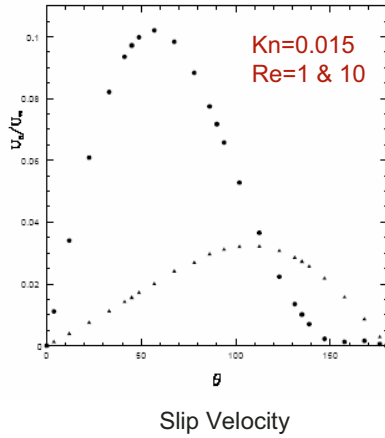
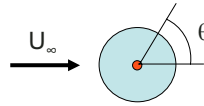
Ahmed & Beskok, 2002

Conclusions

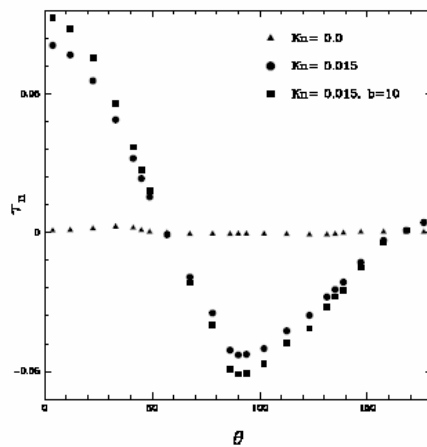
- Velocity slip and temperature jump increase with the Knudsen number.
- Drag reduction, due to Rarefaction (both pressure-drag and skin friction).
- Viscous-drag can be as high as 50% of the pressure-drag. Hence it is an important factor to be considered in design.
- Large density variations across the geometry are due to compressibility.
- Viscous heating causes significant heat generation → heat transfer

External Flows

Flow Past a Cylinder



Flow Past a Cylinder



In slip surfaces the viscous normal stresses achieve finite values and increase proportional to the Knudsen number

The total normal stress (viscous normal stresses and pressure) do not vanish as the rarefaction effects increase

Flow Past a Sphere (External Flow)

$$F_D = 6\pi\mu UR, \quad \text{Stokes Drag} \qquad C_D = \frac{F_D}{\frac{1}{2}\rho U^2 \pi R^2} = \frac{12\mu}{\rho UR} = \frac{12}{Re},$$

$$F_D = 6\pi\mu UR \left(\frac{1 + 4\frac{2-\sigma}{\sigma} Kn}{1 + 6\frac{2-\sigma}{\sigma} Kn} \right) \quad Kn < 0.1, \text{ Emerson \& Barber, 2002}$$

Skin-friction drag:

$$F_{SF} = 4\pi\mu UR \left(\frac{1}{1 + 6\frac{2-\sigma}{\sigma} Kn} \right).$$

Drag force due to the viscous normal stresses:

$$F_{SN} = 4\pi\mu UR \left(\frac{4\frac{2-\sigma}{\sigma} Kn}{1 + 6\frac{2-\sigma}{\sigma} Kn} \right).$$

Pressure or form drag:

$$F_{PD} = 2\pi\mu UR \left(\frac{1 + 4\frac{2-\sigma}{\sigma} Kn}{1 + 6\frac{2-\sigma}{\sigma} Kn} \right).$$

Sphere in a Pipe

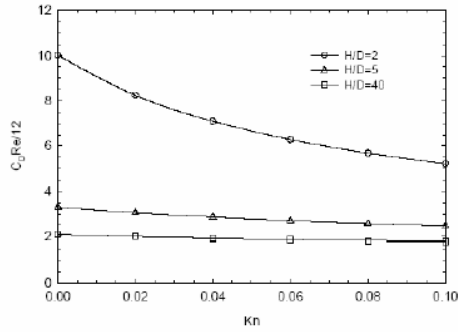
Stokes Flow, Sphere moving in a pipe w/ velocity U (Haberman & Sayre, 1958)

$$F_D = \frac{6\pi\mu UR \left(1 - 0.75857\left(\frac{D}{H}\right)^5 \right)}{\left(1 - 2.1050\frac{D}{H} + 2.0865\left(\frac{D}{H}\right)^3 - 1.7068\left(\frac{D}{H}\right)^5 + 0.72603\left(\frac{D}{H}\right)^6 \right)}$$

Stokes Flow, Stationary sphere in a pipe with maximum flow velocity U

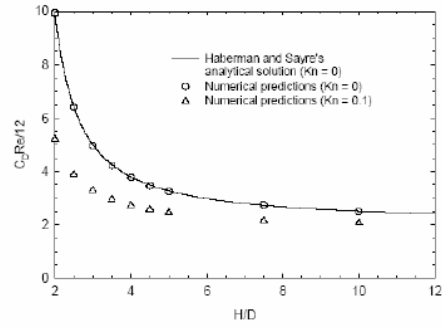
$$F_D = \frac{6\pi\mu UR \left(1 - \frac{2}{3}\left(\frac{D}{H}\right)^2 - 0.20217\left(\frac{D}{H}\right)^5 \right)}{\left(1 - 2.1050\frac{D}{H} + 2.0865\left(\frac{D}{H}\right)^3 - 1.7068\left(\frac{D}{H}\right)^5 + 0.72603\left(\frac{D}{H}\right)^6 \right)}$$

Sphere in a Pipe



Variation of normalized total drag as a function of the Kn

$$C_D = \frac{F_D}{\frac{1}{2}\rho U^2 \pi R^2} = \frac{12\mu}{\rho U R} = \frac{12}{Re}$$



Variation of normalized total drag as a function of the blockage at Kn=0.1

